Why Do Cysteine Dioxygenase Enzymes Contain a 3-His Ligand Motif Rather than a 2His/1Asp Motif Like Most Nonheme Dioxygenases?

Sam P. de Visser*,† and Grit D. Straganz‡

The Manchester Interdisciplinary Biocenter and the School of Chemical Engineering and Analytical Science, The University of Manchester, 131 Princess Street, Manchester, M1 7DN, United Kingdom, and Graz University of Technology, Institute of Biotechnology and Biochemical Engineering, Petersgasse 12, A-8010 Graz, Austria

Received: November 3, 2008; Revised Manuscript Received: December 22, 2008

Density functional theory calculations on the oxygen activation process in cysteine dioxygenase (CDO) and three active site mutants whereby one histidine group is replaced by a carboxylic acid group are reported. The calculations predict an oxygen activation mechanism that starts from an $Fe^{III}-O-O^{\bullet}$ complex that has close lying singlet, triplet, and quintet spin states. A subsequent spin state crossing to the quintet spin state surfaces leads to formation of a ring-structure whereby an O−S bond is formed. This weakens the central O−O bond, which is subsequently broken to give sulfoxide and an iron−oxo complex. The second oxygen atom is transferred to the substrate after a rotation of the sulfoxide group. A series of calculations were performed on cysteine dioxygenase mutants with a 2His/1Asp motif rather than a 3His motif. These calculations focused on the differences in catalytic and electronic properties of nonheme iron systems with a 3His ligand system versus a 2His/1Asp motif, such as taurine/α-ketoglutarate dioxygenase (TauD), and predict why CDO has a 3His ligand system while TauD and other dioxygenases share a 2His/1Asp motif. One mutant (H86D) had the ligand trans to the dioxygen group replaced by acetate, while in another set of calculations the ligand trans to the sulfur group of cysteinate was replaced by acetate (H88D). The calculations show that the ligands influence the spin state ordering of the dioxygen bound complexes considerably and in particular stabilize the quintet spin state more so that the oxygen activation step should encounter a lower energetic cost in the mutants as compared to WT. Despite this, the mutant structures require higher O−O bond breaking energies. Moreover, the mutants create more stable iron−oxo complexes than the WT, but the second oxygen atom transfer to the substrate is accomplished with much higher reaction barriers than the WT system. In particular, a ligand trans to the sulfur atom of cysteine that pushes electrons to the iron will weaken the Fe−S bond and lead to dissociation of this bond in an earlier step in the catalytic cycle than the WT structure. On the other hand, replacement of the ligand trans to the dioxygen moiety has minor effects on cysteinate binding but enhances the barriers for the second oxygen transfer process. These studies have given insight into why cysteine dioxygenase enzymes contain a 3His ligand motif rather than 2His/1Asp and show that the ligand system is essential for optimal dioxygenation activity of the substrate. In particular, CDO mutants with a 2His/1Asp motif may give sulfoxides as byproduct due to incomplete dioxygenation processes.

Introduction

Oxygen activating enzymes have important functions in biosystems ranging from drug metabolism, the biosynthesis of hormones, and detoxification processes.[1] Due to their versatility, regioselectivity, and efficiency these enzymes are of great interest to the biotechnology industry. Understanding the factors that determine their reactivity patterns has been the topic of numerous studies through, e.g., enzyme properties, mutations, and the creation of synthetic analogues (biomimetics) that resemble the activity and properties of enzymes.[2] Oxygen activating enzymes can roughly be divided into two classes: heme and nonheme enzymes. In this work we will focus on mononuclear nonheme enzymes and in particular on the ligand effects on the oxygenation properties of the metal center. Two important nonheme enzymes with functions for human health are cysteine dioxygenase (CDO) and taurine/α-ketoglutarate dioxygenase (TauD), which are the topic of this study.

SCHEME 1: Conversion of Cysteine to Cysteine Sulfinic Acid by CDO Enzymes

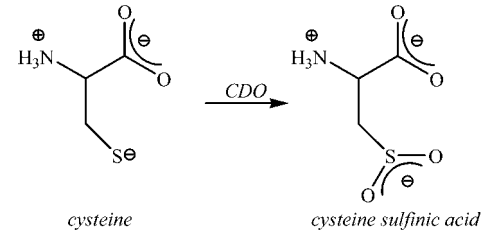

cysteine *cysteine sulfinic acid*

CDO is a nonheme iron enzyme that catalyzes the first step in the metabolism of cysteine in the body (Scheme 1) thereby converting it into cysteine sulfinic acid.[3] Cysteine is a nonessential amino acid that is synthesized in the body from methionine; however, it is toxic in high concentrations and a series of enzymes starting with CDO are involved in its metabolism. Loss of CDO activity in the body has been

* Corresponding author. E-mail: sam.devisser@manchester.ac.uk. Phone: +44-161-3064882. Fax: +44-161-3065201.
† The University of Manchester.
‡ Graz University of Technology.

10.1021/jp809700f CCC: $40.75
Published on Web 02/06/2009

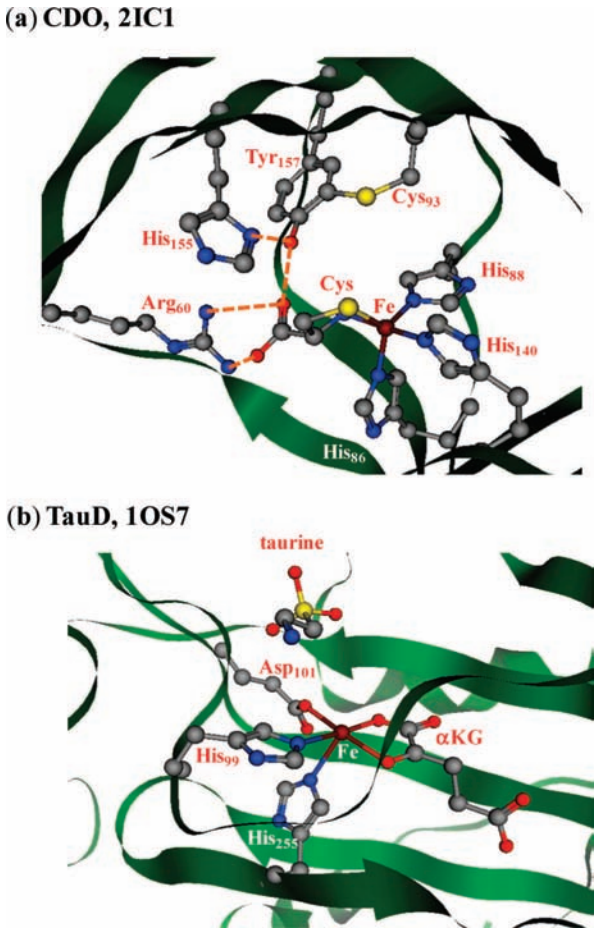

Figure 1. Extracts of the active site structures of CDO (top) and TauD (bottom) enzymes as taken from the 2IC1 and 1OS7 pdb files. All amino acids are labeled as in the pdb files.

correlated with such diseases as Alzheimer's and Parkinson's,[4] as well as with a neurological disorder associated with iron accumulation leading to a decline in CDO activity.[5] Therefore, CDO enzymes catalyze an important and crucial bioprocess in the body vital for human health. Despite the importance of this enzyme for human health only a few experimental studies on catalytic cycle intermediates are reported and a single theoretical study on the oxygen activation mechanism.[6−8] Unresolved issues in CDO activity relate, e.g., to the oxygenation process, the function of the ligands bound to the metal and the (predominantly polar) secondary sphere amino acids.

The active center of CDO enzymes is shown in Figure 1 as taken from the 2IC1 pdb file, which is a substrate bound complex.[7] CDO is a nonheme iron enzyme of which the metal is bound to the protein backbone via three linkages with histidine groups (His_{86}, His_{88}, and His_{140}). Two of the remaining three ligand sites of the metal are occupied by substrate cysteine that binds as a bidentate ligand. It has been anticipated that the sixth ligand site is reserved for dioxygen binding that initiates the dioxygenation process leading to cysteine sulfinic acid products.[7] Experimental studies with $^{18}O_2$ showed that both oxygen atoms of molecular oxygen are incorporated into cysteine sulfinic acid products.[9] Note that the substrate is locked in a rigid conformation through a salt bridge with a neighboring arginine residue (Arg_{60}) as well as through a network of hydrogen bonds that involve the Tyr_{157}, Cys_{93}, and His_{155} residues. An interesting feature of the active site of CDO is the covalent linkage of Tyr_{157} with Cys_{93} that should keep the aromatic ring of Tyr_{157} in a constraint orientation in the active site. It is currently unclear what the function of this covalent linkage is but it does not seem essential for catalytic activity although at physiologically relevant cysteine concentrations it did increase the catalytic efficiency by 10-fold.[10]

TauD is a closely related enzyme to CDO and structurally shows many similarities.[11] TauD belongs to the class of α-ketoacid dioxygenases, which are nonheme enzymes involved in, e.g., the biosynthesis of collagen in mammals and antibiotics in microbes.[12] Furthermore, in this class of enzymes also the AlkB repair enzymes are included that catalyze the demethylation of alkylated DNA and RNA strands.[13] TauD binds α-ketoglutarate (αKG) and molecular oxygen on an iron center and taurine in its vicinity. During the catalytic cycle, one of the oxygen atoms of molecular oxygen is transferred to αKG to give succinate, carbon dioxide, and an iron(IV)−oxo active oxidant that subsequently hydroxylates taurine. The active site structure as depicted in Figure 1b is taken from the 1OS7 pdb file.[14] Thus, TauD is a nonheme iron enzyme where the metal is bound to the protein via interactions with two histidines (His_{99} and His_{255}) and a carboxylic acid group of Asp_{101} in a 2His/1Asp structural motif.[15] Of the remaining three ligand sites of iron, two are occupied by αKG substrate that binds as a bidentate ligand, while the last binding site (vacant in Figure 1b) is reserved for molecular oxygen.

Extensive studies of nonheme biomimetics with a structural and functional *N*,*N*,*O*-motif that resembles the 2His/1Asp motif in dioxygenases have been reported.[2c,16] It was shown that these biomimetic systems are efficient oxidants of olefin epoxidation and cis-dihydroxylation reactions. However, it appears that the carboxylic acid group is not essential to retain the catalytic efficiency of the iron center as nonheme biomimetics with pentacoordinated ligands that bind via five Fe−N linkages give more efficient hydroxylation or epoxidation reactions.[17] Recently, biomimetic studies were reported that specifically addressed the effects of ligands on a nonheme iron(IV)−oxo system, whereby the iron is ligated to a tetradentate ligand and the sixth binding site of the metal is occupied with variable ligands.[18,19] Two typical tetradentate ligands were investigated: TMC (TMC = 1,4,8,11-tetramethyl-1,4,8,11-tetraazacyclotetradecane) and TPA (TPA = tris(2-pyridylmethyl)amine). The TMC ligand has four nitrogen atoms located in one plane of symmetry that bind to the metal, so that the oxo group is located opposite the variable ligand (the axial ligand). By contrast, in TPA the four coordinated nitrogen atoms are located in a tetrahedron on one side of the iron, which means that the oxo and variable ligand are perpendicular to each other. These two ligand orientations have been designated as trans and cis ligands and give the corresponding trans and cis effects of the ligand on the oxidant. Thus, studies of the axial ligand effect using an iron(IV)−oxo(TMC) complex with variable axial ligand L = CH_3CN, CF_3COO^-, and N_3^- showed that the oxo-transfer reaction to PPh_3 is influenced by the push effect of the axial ligand that enhances the electrophilicity of the iron−oxo group. Generally, the effect of ligands trans to the oxo group is significant, while the cis ligand has a different but smaller effect. These studies are in line with earlier studies with an iron(IV)−oxo group in a porphyrin environment, such as tetramesitylporphyrin.[20] For example, the axial ligand was shown to entice a trans effect due to the fact that some ligands stabilize Fe^{III} intermediates rather than Fe^{IV} intermediates.

It appears, therefore, that ligands bound to a metal center have variable effects on substrate monoxygenation and dioxygenation. To gain insight into the nature of the ligand environment in CDO enzymes, we have performed a series of density

functional theory (DFT) studies on an active site model of CDO, whereby one of the histidine ligands of iron is replaced by an acetic acid group to give the system a 2His/1Asp bound motif. Experimental mutagenesis studies of this kind are often prohibited by the loss of a cofactor or the destabilization of protein structure[21] that accompanies the respective mutations through outer sphere effects. In the rare cases where the successful conversion of a 2His/1carboxylate center to its 3His counterpart was reported, marked decreases in activity were found.[22] DFT calculations, such as those reported in this work, constitute a tool to study the impact of the first and second coordination sphere of the active site of enzymes and predict the impact of secondary effects caused by the protein structure.

The studies were aimed at resolving the issue, why CDO has the rare 3His bound motif and what would happen to the dioxygenation reaction if this motif was replaced by a 2His/1Asp motif that is characteristic for the α-ketoacid dioxygenases. In principle, the three different 2His/1Asp mutants (H86D, H88D, and H140D) are expected to give different effects due to the location of each histidine group in the enzyme active site and result from differences in cis and trans effects of ligands. The studies show that the 3His structural motif in CDO is essential for optimal dioxygenation activity due to destabilizing effects of negatively charged ligands.

Methods

The calculations presented here were done using well-established procedures and methods similar to previous calculations of our group on CDO and TauD enzymes.[8,23] We use the UB3LYP hybrid density functional method[24] as it is known to reproduce experimental rate constants and kinetic isotope effects with good accuracy and predict reaction energies and barriers with good reproducibility.[25] The iron is described with a Los Alamos-type double-ζ quality LACVP basis set, while all other atoms are represented by a 6-31G basis set (basis set B1).[26] Full optimizations were performed in Jaguar 7.0 followed by an analytical frequency in Gaussian-03.[27,28] Subsequent single point calculations with a triple-ζ quality LACV3P+ basis set on iron and 6-311+G* on the rest of the atoms were done to correct the energies (basis set B2). Energies reported in this work are taken from the UB3LYP/B2 calculations with zero-point corrections at UB3LYP/B1. To test the effect of the environment on the reaction barriers we ran single point calculations in Jaguar 7.0 using the self-consistent reaction field model with a dielectric constant of $\varepsilon = 5.7$ and a probe radius of 2.72 Å. These values have been shown to be a good representation of the polarized environment of an enzyme mimicked system.[29] Group spin densities and charges were taken from the Mulliken populations.

The model of the active site of CDO was taken from the 2IC1 pdb file, which is a substrates bound complex of human CDO.[7] We use a large active site model of 81 atoms that contains all important features of the enzyme including several second sphere amino acids that form key hydrogen bonding interactions with the substrate and iron ligands (Scheme 2). Thus, cysteine binds at an iron center that is bound to the protein through three histidine ligands (His_{86}, His_{88}, and His_{140}), which we abbreviated to imidazole. The carboxylic acid group of cysteine is locked in a salt bridge with an arginine side chain (Arg_{60}), which we abbreviated to methylguanidinium. A nearby tyrosine residue (Tyr_{157}) donates a hydrogen bond to this salt bridge and its hydroxyl group accepts a hydrogen bond from another histidine group (His_{155}). This tyrosine group is in a fairly rigid conformation as in addition to these hydrogen bonding interactions it also is linked via a covalent bond with the side chain of Cys_{93}. The essential features of these groups have been taken into the model: histidine groups were abbreviated to imidazole (His_{86}, His_{88}, His_{140}, His_{155}), tyrosine was replaced by phenol and, Cys_{93} was replaced by methyl mercaptane. Careful analysis of the pdb structure implicated no hydrogen bonding donors to the His_{155} side chain except from Tyr_{157}, therefore His_{155} was abbreviated to imidazole rather than imidazolate or protonated imidazole. The structure of these groups was initially taken from the 2IC1 pdb[7] file and hydrogen atoms and molecular oxygen were added to create a system with stoichiometry $FeC_{24}N_{12}H_{37}S_2O_5$ and overall charge +1. To prevent the system from undergoing unnatural changes with respect to the crystal structure we fixed one carbon atom of Arg_{60}, His_{155}, and Tyr_{157} as identified with a star in Scheme 2. The calculations on this model are labeled with a subscript WT representing wild-type CDO.

SCHEME 2: CDO Model As Used in These Studies Whereby Atoms Labeled with a Star Were Fixed during the Optimizations[a]

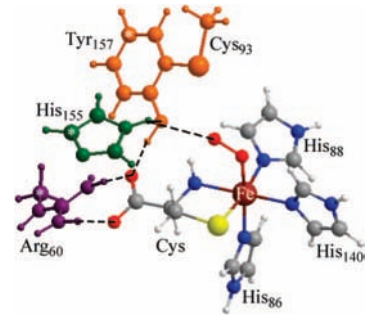

[a] In the H88D, H86D, and H140D mutants the respective imidazole groups were replaced by acetate.

In a subsequent set of calculations we investigated three CDO mutants with a 2His/1Asp motif mimicking the active site of TauD: one whereby the axial histidine ligand (i.e., trans to the oxygen group) was replaced by acetic acid (designated H86D mutant), another one where the histidine group trans to the sulfur atom of cysteine was replaced by acetic acid (designated H88D mutant), and finally one where the histidine group trans to the amide group of cysteinate was replaced by acetic acid (designated H140D mutant). The dioxygen activation process leading to cysteine sulfinic acid was calculated for WT as well as the H86D and H88D mutants.

The calculations produced a large amount of data that we cannot include in the paper for space economy, but all obtained results are given in the Supporting Information, while we will focus only on the major trends here.

Results

CDO has a unique ligand system where the metal in the active site is bound to three histidine groups that connect it to the protein backbone. By contrast, many nonheme iron containing enzymes have a characteristic 2His/1Asp motif instead.[2] To gain insight into what the effect of a 2His/1Asp ligand motif is on the catalytic properties of nonheme enzymes, we studied the oxygen activation process of CDO enzymes and its H86D and H88D mutants, i.e., an enzyme with a 3His motif vis-à-vis a 2His/1Asp motif. Scheme 2 displays the enzyme model that has been used in our studies presented here.

Catalytic Cycle of CDO Enzymes. Let us first summarize the dioxygen activation process of wild-type CDO as obtained with DFT calculations.[8] Scheme 3 displays the reaction mech-

SCHEME 3: Reaction Mechanism of Dioxygen Activation by CDO Enzymes and the Dioxygenation of Cysteine

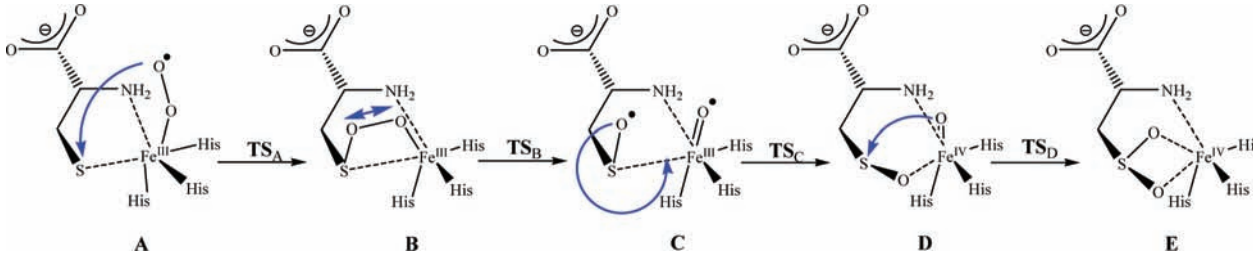

anism for the dioxygen activation in WT-CDO starting from the dioxygen bound complex (**A**) with the reaction coordinates of each step in the catalytic mechanism identified. The mechanism starts from the resting state with the metal in oxidation state Fe^{II} in a stepwise mechanism via an initial attack of the terminal oxygen atom of O_2 on the sulfur atom of cysteinate to form a ring structure (**B**) with an Fe−O−O−S four-membered ring via a transition state $\mathbf{TS}_A$. In a subsequent step the dioxygen bond breaks via barrier $\mathbf{TS}_B$ to form a *cis*-sulfoxide species **C**. Thereafter an internal rotation around the C−C bond of cysteine via barrier $\mathbf{TS}_C$ creates the *trans*-sulfoxide **D**. When that happens, the sulfur group is accessible again to the remaining oxygen atom of the iron−oxo group and the second oxygenation reaction takes place via barrier $\mathbf{TS}_D$ to form cysteine sulfinic acid products **E**.

Although the mechanism was reported in ref 8, we did additional calculations that took the effect of the environment into consideration using a dielectric constant of $\varepsilon = 5.7$ and the results are shown in Figure 2. To distinguish the structures for the WT from those in the mutants, all labels for the WT structure contain the subscript "WT". As often is the case with transition metal systems, each intermediate can appear in several low-lying spin state structures, leading to multistate reactivity patterns.[30] Therefore we calculated the complete reaction mechanism on the lowest lying singlet, triplet, quintet, and septet spin state surfaces in the gas phase. The dioxygen bound species has a singlet spin ground state with $^3\mathbf{A}_{WT}$ and $^5\mathbf{A}_{WT}$ higher in energy by 2.6 and 5.9 kcal mol^{-1}, respectively. The dioxygen activation barrier ($\mathbf{TS}_A$) leading to the ring structure ($\mathbf{B}_{WT}$), however, is the lowest on the quintet spin state surface. This quintet spin state remains the lowest lying state for the rest of the reaction mechanism. For clarity, however, we only show the quintet spin state surface for the rest of the reaction mechanism; details of the other spin state surfaces are given in ref 8. Thus, it is expected that the reaction starts with a singlet to quintet spin state crossing leading to $^5\mathbf{B}_{WT}$. The quintet spin state surface shows some interesting features, namely, each subsequent intermediate is lower in energy than its precursor. In addition, the same applies to each transition state, with the first step being rate determining in the oxygen activation process. Thus, the first barrier is the largest (15.9 kcal mol^{-1} from $^1\mathbf{A}_{WT}$ to $^5\mathbf{TS}_{A,WT}$), while $^5\mathbf{TS}_{B,WT}$, $^5\mathbf{TS}_{C,WT}$, and $^5\mathbf{TS}_{D,WT}$ are only 8.2, 4.0, and 0.4 kcal mol^{-1}, respectively, in the gas phase. This mechanism implies that most intermediates after dioxygen binding will have a short lifetime and dioxygen activation via $\mathbf{TS}_A$ will be rate determining. Addition of a dielectric constant to the structures gives only minor changes to the energies of the various intermediates, and the reaction mechanism stays the same. This implies that the hydrophilic nature of the binding pocket/active site does not influence the reaction barriers and the dioxygenation mechanism.

Catalytic Cycle of H86D and H88D Mutants. The potential energy profiles of two CDO mutants with a 2His/1Asp motif, H86D and H88D, are shown in Figure 3. These mutants have an acetate group mimicking an Asp ligand in the axial ligand position, i.e., trans to the dioxygen group (in H86D), or trans to the sulfur atom (in H88D). The structures of the intermediates and transition states are labeled as those in Figure 2, with the ones for the H86D mutant with subscript "A" while those for the H88D mutant with "M". As follows from the potential energy profiles shown in Figure 3 both mutants are able to dioxygenate cysteine to cysteine sulfinic acid with similar exothermicity as the WT system. However, in both mutants the rate determining step is not the dioxygen activation step via $^5\mathbf{TS}_A$ anymore as was the case for the WT system: In the H88D mutant the rate determining step is the attack of the second oxygen atom on the sulfur atom via barrier $^5\mathbf{TS}_{DM}$, while in the H86D mutant the dioxygen bond breaking barrier $^5\mathbf{TS}_{BA}$ is rate

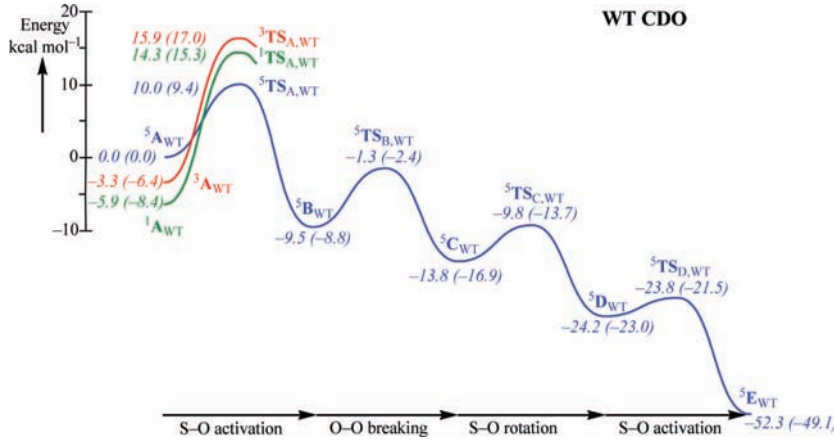

Figure 2. Potential energy profile for the dioxygenation of cysteine by WT CDO enzymes. All energies are in kcal mol^{-1} relative to $^5\mathbf{A}_{WT}$ and taken from the UB3LYP/B2//UB3LYP/B1 calculations with ZPE at the UB3LYP/B1 level of theory. Values in parentheses were obtained in a dielectric constant of $\varepsilon = 5.7$. The reaction coordinates at each step are as identified in Scheme 3.

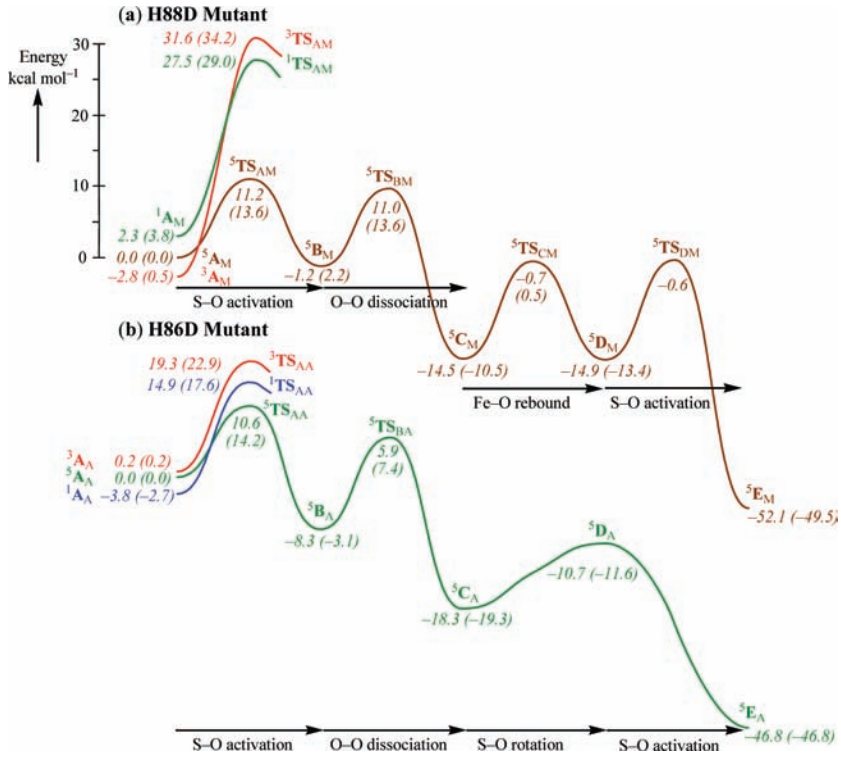

Figure 3. Potential energy profiles for the dioxygenation of cysteine by H88D and H86D mutants of CDO. All energies are in kcal mol^{-1} relative to ^{5}**A** and taken from the UB3LYP/B2//UB3LYP/B1 calculations with ZPE at the UB3LYP/B1 level of theory. Values in parentheses were obtained in a dielectric constant of $\varepsilon = 5.7$.

determining. Below we will discuss the geometries and the reasons why this has changed.

The dioxygen bound species of H86D and H88D mutants similarly to WT CDO have several close-lying spin states with multiplicity singlet, triplet, and quintet spin. In H88D the triplet spin state (^{3}**A**$_M$) is the ground state with the quintet spin state only 2.8 kcal mol^{-1} higher in energy. However, the dioxygen activation barriers leading to ^{1,3,5}**B**$_M$ are much higher in energy on the singlet and triplet spin state surfaces than on the quintet spin state where a barrier of 11.2 kcal mol^{-1} is found. Consequently, a spin state crossing from the triplet to the quintet spin state surface will be required prior to the oxygen activation process. The rest of the reaction mechanism, similarly to WT, is on a dominant quintet spin state surface. Likewise, in the H86D mutant the ground state is in the singlet spin state, while the triplet and quintet spin states are 4.0 and 3.8 kcal mol^{-1} higher in energy, respectively. Also for the H86D mutant a spin state crossing to the quintet spin state surface is required during the dioxygen activation, which has the lowest barriers and most stable intermediates in the rest of the mechanism.

Although **B** is lower in energy than the dioxygen bound complexes for both mutants, the exothermicity of the H88D mutant to form ^{5}**B**$_M$ is significantly smaller. More importantly, the dioxygen bond breaking via barriers ^{5}**TS**$_{BA}$ and ^{5}**TS**$_{BM}$ costs significantly more energy for the mutants as compared to the WT enzyme. Thus, in the WT a barrier of 8.2 kcal mol^{-1} for the O−O bond breaking is required, while in the H88D and H86D mutants the barriers are 12.2 and 14.2 kcal mol^{-1}, respectively. Moreover, ^{5}**TS**$_{B,WT}$ is lower in energy than ^{5}**A**$_{WT}$ whereas the corresponding barriers for the two mutants are higher in energy than the dioxygen bound complexes. In particular, in the H88D mutant the two barriers ^{5}**TS**$_{AM}$ and ^{5}**TS**$_{BM}$ are of similar energy.

Dissociation of the dioxygen bond gives a cysteinyl oxide intermediate (**C**) in an exothermic process. Interestingly, this *cis*-sulfoxide intermediate is much more stable in the mutants than it is in the WT complex. In the WT system the reaction mechanism from the cysteinyl oxide intermediate (**C**) is highly exothermic with very small barriers. By contrast the mutants experience high barriers and only after ^{5}**TS**$_D$ does the reaction gain significant energy to give cysteine sulfinic acid in a high exothermicity. Therefore, the reactions for the mutants will be much slower with lower rate constants. In the H88D mutant the cysteinyl oxide intermediates ^{5}**C**$_M$ and ^{5}**D**$_M$ are of equal energy, while ^{5}**D**$_A$ is higher in energy than ^{5}**C**$_A$. Moreover, this mutant has negligible barriers ^{5}**TS**$_{CA}$ and ^{5}**TS**$_{DA}$ so that the second oxygenation, i.e., from ^{5}**D**$_A$ to ^{5}**E**$_A$, will be spontaneous.

Let us now go in more detail over the geometric differences of the mutants as compared to the WT structures in order to find out what the reasons for the change in rate determining steps are. Optimized geometries of wild-type, H86D mutant and H88D mutant of the catalytic cycle intermediates are shown in Figures 4−6. The structures only show the essential features of the iron with its direct ligands while the secondary amino acids Arg$_{60}$, Cys$_{93}$, His$_{155}$, and Tyr$_{157}$ that are also part of the model have been omitted from the structures for clarity. Full geometries of all structures are shown in the Supporting Information, but since the hydrogen bonds between the various residues do not change a lot along the reaction mechanism we will focus only on the structural features that do encounter changes.

The dioxygen bound reactant complexes ^{5}**A**$_{WT}$, ^{5}**A**$_M$, and ^{5}**A**$_A$ are shown in Figure 4. As can be seen, replacement of one of the histidine groups by acetate has a drastic effect on the optimized geometries. Thus, the three histidine groups form a Fe−N bond with the metal of 2.128−2.197 Å in the WT structure. With the axial histidine ligand replaced by aspartic acid as in ^{5}**A**$_A$ the two remaining Fe−N bonds of iron with histidine groups have decreased to 2.034 and 2.063 Å. By contrast, in the H88D mutant the axial Fe−N distance is

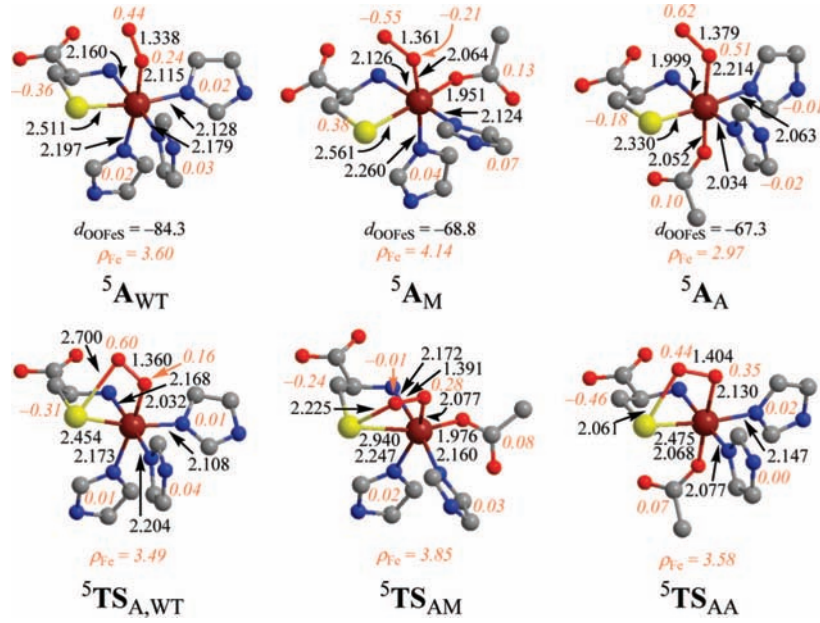

Figure 4. Extracts of optimized geometries (UB3LYP/B1) of the dioxygen bound complexes (^{5}**A**) and the oxygen activating transition states (^{5}**TS**$_A$) of WT, H88D, and H86D. All bond lengths are given in angstroms and group spin densities in pink and italics. Second sphere amino acids (Arg_{60}, Cys_{93}, His_{155}, and Tyr_{157}) and hydrogen atoms have been omitted for clarity.

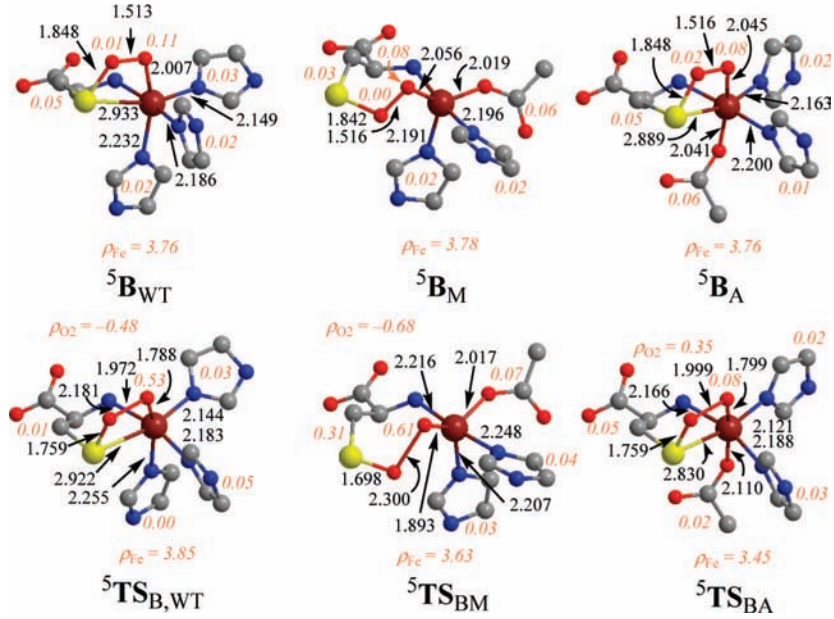

Figure 5. Extracts of optimized geometries (UB3LYP/B1) of the dioxygen bridged complexes (^{5}**B**) and the dioxygen bond breaking transition states (^{5}**TS**$_B$) of WT, H88D, and H86D. All bond lengths are given in angstroms and group spin densities in pink and italics. Second sphere amino acids (Arg_{60}, Cys_{93}, His_{155}, and Tyr_{157}) and hydrogen atoms have been omitted for clarity.

elongated to 2.260 Å. This mutant binds cysteine as strong as the WT enzyme with similar Fe−S and Fe−NH_2 distances. With the axial histidine replaced by aspartic acid a different picture emerges, where the cysteine is much stronger bound and the Fe−S and Fe−NH_2 distances are well shorter than in the WT enzyme. This does not seem to affect the dioxygen activation process as similar barriers are observed with respect to the other models.

The terminal oxygen atom of the dioxygen bound species (**A**) attacks the sulfur atom of cysteinate to form a four-membered ring (Fe−O−O−S ring) via a transition state **TS**$_A$. Optimized geometries and group spin densities of ^{5}**TS**$_{A,WT}$, ^{5}**TS**$_{AM}$, and ^{5}**TS**$_{AA}$ are displayed in Figure 4. In all three systems the dioxygen activation leads to a ring structure with barrier heights of the same order of magnitude (10.0−11.2 kcal mol^{-1}). Notwithstanding the similarities in barrier heights there are some large geometric and electronic differences between the three individual structures. Thus, in ^{5}**TS**$_{A,WT}$ the transition state is early, i.e., geometrically closer to ^{5}**A**$_{WT}$ than to ^{5}**B**$_{WT}$ with a long O−S distance and short O−O and Fe−O distances. By contrast, geometrically ^{5}**TS**$_{AA}$ is product-like in geometry with short S−O and long O−O and Fe−O distances. Nevertheless, the iron−sulfur bond is of almost equal strength in WT and H86D mutant, whereas it is considerably weakened in ^{5}**TS**$_{AM}$ to 2.940 Å. In the WT structure there is little electronic rearrangement along the pathway from ^{5}**A**$_{WT}$ to ^{5}**TS**$_{A,WT}$: the dioxygen moiety retains 0.76 spin density, $\rho_{Fe} = 3.49$, and the cysteinate group has −0.31 spin density. In the mutant with the axial ligand replaced by a carboxylic acid group the spin densities in the transition state resemble those for the WT. A

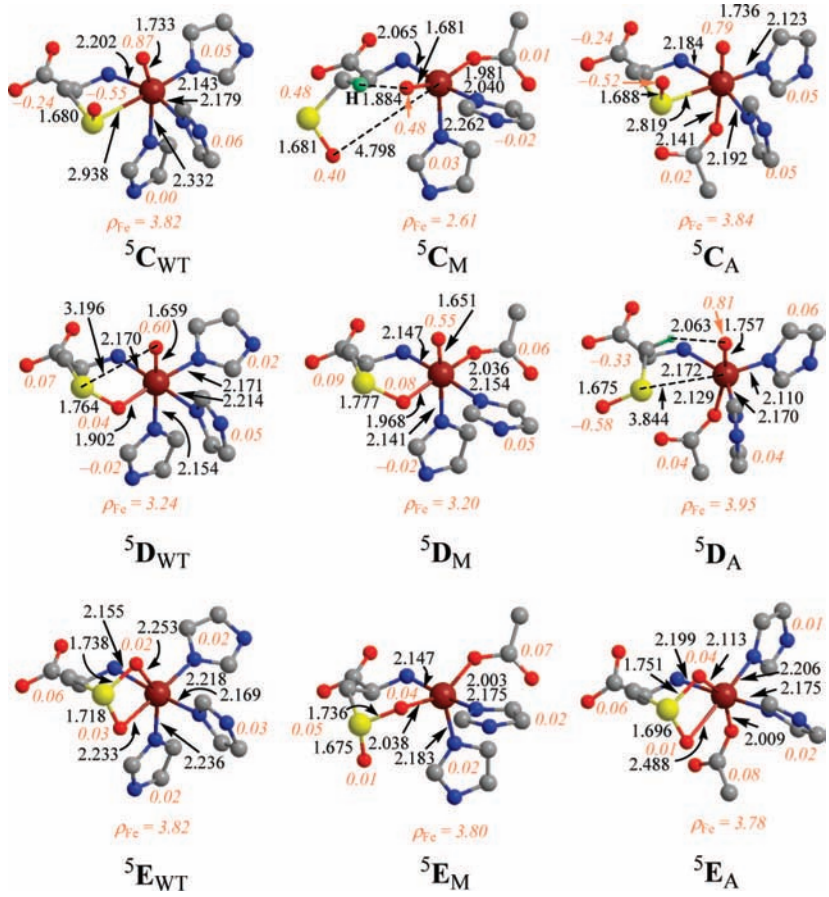

Figure 6. Extracts of optimized geometries (UB3LYP/B1) of the *cis*-sulfoxide (^{5}**C**), *trans*-sulfoxide (^{5}**D**), and cysteine sulfinic acid product complexes (^{5}**E**) of WT, H88D, and H86D. All bond lengths are given in angstroms and group spin densities in pink and italics. Second sphere amino acids (Arg_{60}, Cys_{93}, His_{155}, and Tyr_{157}) and hydrogen atoms have been omitted for clarity.

totally different picture has emerged in ^{5}**TS**$_{AM}$, where the dioxygen group lost almost a full electron in spin density and the iron has four unpaired electrons. This electronic situation means that ^{5}**TS**$_{AM}$ already has the orbital occupation of ^{5}**B**$_M$. Indeed a comparison of the group spin densities of ^{5}**TS**$_{AM}$ (Figure 4) and ^{5}**B**$_M$ (Figure 5) shows that the metal has four unpaired electrons and the rest of the groups have no significant spin density. There is still a small amount of unpaired spin density on the oxo group in ^{5}**TS**$_{AM}$ and a similar amount but with opposite sign on the cysteinate group.

After passing the oxygen activating transition state ^{5}**TS**$_A$ the system relaxes to ring structure **B**. Structures ^{5}**B**$_{WT}$ and ^{5}**B**$_A$ are very similar with bond distances and group spin densities of the same order of magnitude. Structure ^{5}**B**$_M$ is completely different from ^{5}**B**$_{WT}$ and ^{5}**B**$_A$, where the Fe−S bond has broken and the dioxygen group bridges the two atoms. Nevertheless, the O−O bond in ^{5}**B**$_M$ is of equal strength as in ^{5}**B**$_{WT}$ and ^{5}**B**$_A$. Despite the difference in dioxygen bridging in ^{5}**B**$_M$ as compared to ^{5}**B**$_{WT}$ all other bond lengths as well as the orbital occupation are the same as in the other structures. Structurally, the O−O bond breaking transition states (^{5}**TS**$_B$) give lengthening of the O−O bond and shortening of the Fe−O and O−S bonds indicative of an oxygen transfer process.

After dioxygen bond breaking a cysteinyl oxide complex (**C**) is formed. This system has considerable radical character on the cysteinyl oxide group of −0.79 (in ^{5}**C**$_{WT}$), 0.88 (in ^{5}**C**$_M$), and −0.76 (in ^{5}**C**$_A$). Geometrically, ^{5}**C**$_M$ has the sulfoxide group displaced from the iron center. This is because the oxo rest group on the iron center is aligned with the carboxylic acid group. Therefore, in the H88D mutant the Fe−S bond is considerably weakened and breaks after the first oxygen atom is transferred from the dioxygen moiety. The oxo rest-group then moves trans to the carboxylic acid group and forms a weak hydrogen bond with a C−H bond of the cysteinyl oxide residue. From this structure, the cysteinyl oxide has to rebind to the iron center in order for the reaction to proceed. This costs a considerable amount of energy as shown above in Figure 3. Geometrically the oxo group needs to move away to its original position perpendicular to the carboxylic acid group. Therefore, considerable structural rearrangement is necessary to convert ^{5}**C**$_M$ into ^{5}**D**$_M$ and as a consequence this step requires a relatively large barrier of 13.8 kcal mol^{-1}. Despite this barrier the system converged back to a structure similar to the WT (^{5}**D**$_{WT}$). In the final reaction step of the H88D mutant the second oxygen atom is transferred via a large barrier to form cysteine sulfinic acid products. Similarly to ^{5}**C**$_M$ also in ^{5}**E**$_M$ the oxo group of the cysteine sulfinic acid group is aligned with the carboxylic acid group. As a result of that only one oxygen atom of cysteine sulfinic acid is bound to the metal while in the WT both oxygen atoms bind to the metal. Thus, in ^{5}**E**$_M$ the metal is five-coordinated, while it is six-coordinated in WT.

In the H86D mutant the cysteinyl oxide intermediate (^{5}**C**$_A$) is similar to the WT structure, but a rotation around the C−C bond does not lead to binding of the oxygen atom to the iron and at the same time significant radical character remains on the cysteinyl oxide group. The final oxygen atom transfer is virtually barrierless and gives cysteine sulfinic acid.

Discussion

In this work we report density functional theory studies on the dioxygen activation process in cysteine dioxygenase and two mutants with a 2His/1Asp structural motif. Few enzymes contain a 3His structural motif, which is expected to give it different properties to systems with a 2His/1Asp bound motif.[3b,31] As shown by experimental and DFT calculations the H99A mutation in TauD led to the loss of a ligand to the metal and its replacement by a water molecule instead as evidenced from spectroscopic studies.[32] The mutant is catalytically active and the mutation is located perpendicular to the Fe−O bond of its active species, i.e. in the cis position. By contrast, the His175Gln mutant of the heme enzyme cytochrome *c* peroxidase only gave a modest effect on the O−O cleavage step in the catalytic cycle but a more pronounced effect on the stabilization of the iron−oxo species.[33] In biomimetic studies the ligand topology was found to have strong influences on the activity of the iron center mainly due to differences in spin state ordering of the active oxidants.[34] Enzyme mutations in silico, as presented in this work, can provide information regarding the effect of ligands on a catalytic center, and the results obtained give knowledge about the fundamental factors that determine reactivity patterns, such as the push/pull effect of ligands, and should explain why CDO has a 3His motif and not a 2His/1Asp structural motif.

WT CDO efficiently transfers both oxygen atoms of molecular oxygen to cysteine substrate.[8] Our studies show that the rate determining step in the process is the initial attack of molecular oxygen on the sulfur of cysteinate to give a peroxo-ring structure ($\mathbf{B}_{WT}$). The calculations indicate that although the singlet spin state is the ground state for the dioxygen bound complex, the rest of the mechanism takes place on a quintet spin surface leading to cysteine sulfinic acid products with large exothermicity. Our DFT studies predict that most intermediates will have a very short lifetime and not accumulate long enough for experimental detection. Nevertheless, the mechanism supports experimental studies that showed that both oxygen atoms of molecular oxygen are incorporated into products. In the next few sections we will describe the effects of site directed mutations in silico on the reaction mechanisms.

Electronic Differences of the Dioxygen Bound Complex of WT and Mutants. Before describing the reasons for the differences in mechanism between WT and CDO mutants, let us first consider the dioxygen binding to a metal center in the various structures. Studies of Morokuma et al.[35] on the analogous enzyme isopenicillin *N* synthase showed that the local environment influences dioxygen bound structures and sometimes changes the spin state ordering, so that an error of a couple of kcal mol^{-1} may be expected in the relative energies of the dioxygen bound complexes. Essentially, the reactivity pattern takes place on a dominant quintet spin state surface, but in none of the systems tested is the quintet spin dioxygen bound species in the ground state. Therefore, a spin state crossing from the ground state in the dioxygen bound complex to the quintet spin state is required. The spin state ordering varies among WT and mutant structures as shown above in Figures 2 and 3. To find out what factors determine the spin state ordering and electron distributions in the systems we analyzed the different dioxygen bound complexes ($\mathbf{A}_{WT}$, $\mathbf{A}_{A}$, and $\mathbf{A}_{M}$) in detail. Consider in Figure 7 the group charges of the optimized geometries of the dioxygen bound complex ($^5\mathbf{A}$) for the WT, H86D, H88D, and H140D systems. The metal has charge $Q = 0.53$ in the WT structure and the dioxygen moiety has charge $Q = -0.20$. All three histidine ligands bear similar overall charge in $^5\mathbf{A}_{WT}$ and

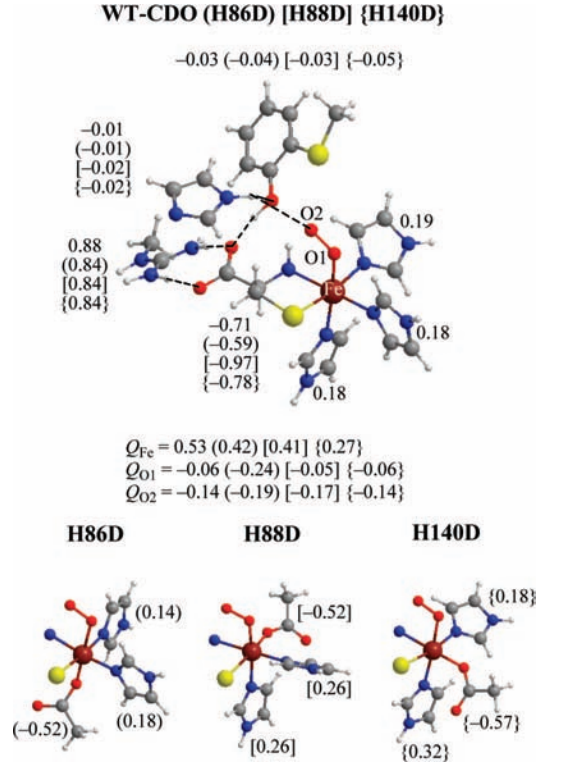

Figure 7. Group charges of dioxygen bound complexes of WT CDO and three His/Asp mutants studied here.

the cysteinate has $Q = -0.71$. Substitution of the histidine group trans to the dioxygen moiety by acetate as in H86D results in withdrawal of charge from the metal to $Q = 0.42$. By contrast, the charge of the histidine groups perpendicular to the acetate group hardly changes, but the dioxygen moiety becomes more anionic ($Q = -0.43$). This also holds true for the H88D and H140D mutants where groups perpendicular to the substituent hardly change in group charge, so that these mutants have an overall charge on the dioxygen group close to that observed for WT. However, the H88D and H140D mutants give a drop in charge on the metal from $Q = 0.53$ in WT to $Q = 0.41$ in H88D and $Q = 0.27$ in H140D. Therefore, an acetate group representing an Asp or Glu in the axial ligand position entices a push effect of electrons toward the iron and dioxygen group. On the other hand, an acetate group in a ligand position perpendicular to the dioxygen moiety (the cis ligands) has little effect on the charges of the O_2 group, but makes the cysteinate more negative instead (in H88D). Therefore, the push effect of a ligand has a strong effect on the charge of its opposite ligand. These observations are in line with biomimetic studies on the cis and trans effects of ligands on an iron−oxo oxidant, which found that trans substitutions can have a considerable effect on the nature of the iron−oxo oxidant through pushing or pulling electron density to/from the iron−oxo group.[36] By contrast, cis substitutions generally give only minor push or pull effects on the iron−oxo group.[36] This push effect of electrons will influence orbital interactions and in the case of the dioxygen bound complex also the spin state ordering of the various electronic states.

The group charges in Figure 7 show that a single mutation in the iron ligand system has drastic effects on the charge distributions of the oxidant; therefore, we analyzed the relevant bonding and antibonding orbitals in detail. These orbital interactions and charge distributions should explain why the spin state ordering in the dioxygen bound complexes varies among

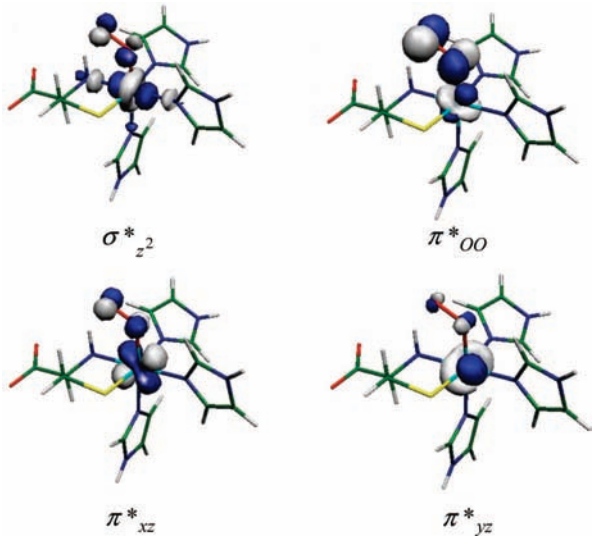

Figure 8. Natural orbitals of $^5\mathbf{A}_{WT}$.

the different systems. The high-lying occupied and low-lying virtual orbitals are determined by the metal 3d orbitals and a pair of antibonding π^* orbitals on the dioxygen moiety (π^*_{OO}). As an example of these orbitals Figure 8 shows the singly occupied molecular orbitals of $^5\mathbf{A}_{WT}$. The lowest lying three 3d orbitals are of π^*-type (π^*_{xy}, π^*_{xz}, and π^*_{yz}) and represent the antibonding interactions of the metal with the dioxygen and axial ligands. Higher lying are a pair of σ^*-type orbitals for the antibonding interactions perpendicular to the Fe−O bond ($\sigma^*_{x^2-y^2}$) and along the O−Fe-axial ligand axis ($\sigma^*_{z^2}$). The ordering of the various spin states is dependent on the relative energies of these individual orbitals and since all orbitals are differently affected by the various ligands bound to the metal this results in significant differences between WT and mutant structures. Electronically, $^5\mathbf{A}_{WT}$ and $^5\mathbf{A}_A$ are described by an $Fe^{III}-O-O^{\bullet}$ system with orbital occupation $\pi^*_{xy}{}^2\ \pi^*_{xz}{}^1\ \pi^*_{yz}{}^1\ \sigma^*_{z^2}{}^1\ \sigma^*_{x^2-y^2}{}^0\ \pi^*_{OO}{}^1$. By contrast, $^5\mathbf{A}_M$ still has an $Fe^{III}-O-O^{\bullet}$ electronic situation but with orbital occupation: $\pi^*_{xy}{}^1\ \pi^*_{xz}{}^1\ \pi^*_{yz}{}^1\ \sigma^*_{z^2}{}^1\ \sigma^*_{x^2-y^2}{}^1\ \pi^*_{OO}{}^1$, i.e., the metal 3d-block is singly occupied and antiferromagnetically coupled to an unpaired electron in π^*_{OO}. As a consequence, the group spin density of the dioxygen moiety in $^5\mathbf{A}_M$ is −0.76, whereas in $^5\mathbf{A}_{WT}$ and $^5\mathbf{A}_A$ it is +0.68 and +1.13, respectively. The enhanced spin density on the dioxygen group in $^5\mathbf{A}_A$ is due to the push effect of electrons of the axial ligand and reflects the increased charge on the group as shown in Figure 7 above.

The substitution of a histidine ligand by acetic acid has a strong effect on the relative energies of the metal 3d orbitals. In particular, the $\sigma^*_{z^2}$ orbital for the antibonding interactions along the O−Fe-axial ligand axis is considerably stabilized with an anionic ligand in the axial position, but also with an anionic ligand trans to the sulfide group of cysteinate. On the other hand, in $^5\mathbf{A}_M$ the $\sigma^*_{x^2-y^2}$ is considerably stabilized due to favorable interactions in the xy-plane of symmetry. As a consequence, the complete metal 3d-block is singly occupied in $^5\mathbf{A}_M$. The π^*_{xy} orbital is destabilized with anionic ligands in $^5\mathbf{A}_A$ and $^5\mathbf{A}_M$, so that the energy gap between the π^*_{xy} and $\sigma^*_{x^2-y^2}$ is reduced in the mutants. It has been shown recently that the $\pi^*_{xy}-\sigma^*_{x^2-y^2}$ orbital energy difference determines the triplet−quintet energy gap of nonheme iron−oxo oxidants.[18c,37] Thus, the push effect of electrons from the axial ligand was shown to decrease the $\pi^*_{xy}-\sigma^*_{x^2-y^2}$ energy difference and thereby favor quintet spin states over triplet spin states. In a similar fashion the same is observed for the dioxygen bound complexes of the CDO

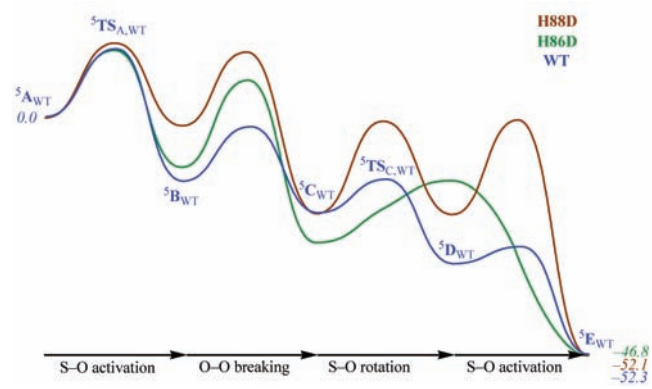

Figure 9. Superimposed potential energy landscapes of WT (blue), H88D (brown), and H86D (green).

mutants, where the push effect of the ligands stabilizes the quintet spin state structures with respect to the singlet and triplet spin state isomers. Consequently, the singlet spin state structure is the ground state in $\mathbf{A}_{WT}$ and is well separated from other spin states, whereas in $\mathbf{A}_A$ and $\mathbf{A}_M$ this state is raised in energy and much closer to the quintet spin state. For the first step in the reaction process a spin state crossing from the singlet to the quintet spin state is required, since $\mathbf{TS}_A$ is the lowest on this spin state surface. Obviously, the lower in energy $^5\mathbf{A}$ is, the easier this spin state crossing will be thereby making $^5\mathbf{TS}_A$ the oxygen activation transition state. Therefore, the mutants are expected to have slightly more efficient dioxygen activation processes from the ground state of $\mathbf{A}$ to $^5\mathbf{B}$. However, in all subsequent reaction steps the WT has significantly lower barriers than the mutant structures. In the next few sections we will go into more detail of the differences encountered between the WT and specific mutants further along the reaction mechanisms.

In the case of TauD the dioxygen bound complex has a triplet spin ground state with the septet and quintet spin states higher in energy by 2.2 and 5.7 kcal mol^{-1}.[38] The oxygen activation barrier for TauD was found to be 10.4 kcal mol^{-1} relative to the dioxygen bound complex in the quintet spin state.[38] At the free energy scale for WT-CDO, however, $^5\mathbf{TS}_A$ is 15.0 kcal mol^{-1} above $^5\mathbf{A}$, which means that the first oxygen activation barrier is well higher in energy for systems with a 3His ligand system compared to those with a 2His/1Asp ligand system. Therefore, CDO enzymes have a 3His ligand system that stabilizes the oxygen atom transfer processes in later steps of the catalytic cycle at the expense of the initial oxygen activation step.

What Happens to the Catalytic Mechanism of CDO if the 3His Motif Is Replaced by 2His/1Asp? To understand the differences between WT and CDO mutants we present in Figure 9 all potential energy surfaces superimposed. As follows, the initial S−O activation starting from a dioxygen bound complex ($\mathbf{A}$) undergoes comparable barriers of 10.0−11.2 kcal mol^{-1}. However, in the H88D mutant this does not lead to a ring-structure but rather a linear peroxo-sulfide bound system ($^5\mathbf{B}_M$). Thus, the push effect of the anionic ligand trans to the Fe−S bond weakens this bond and prevents formation of the ring-structure. Obviously, due to the loss of the Fe−S bond $^5\mathbf{B}_M$ is destabilized with respect to $^5\mathbf{B}_{WT}$. The charge and spin distribution (Figure 5) destabilizes the mutant barriers for O−O bond breakage and raises them in energy. However, an anionic ligand trans to an iron−oxo group leads to stabilization of this complex, hence $^5\mathbf{C}_A$ is stabilized over $^5\mathbf{C}_{WT}$. The reaction mechanism for the H88D mutant diverges from here as the sulfoxide group has lost contact with the metal. Therefore, a rebound step to

bring the group close to the iron−oxo group is required, which costs a significant amount of energy. The final oxygen atom transfer gives product complexes with an overall exothermicity close to that obtained for the WT structure. In the H86D mutant, by contrast, the reaction starting from $^5\mathbf{C}_A$ led to release of sulfoxide from the metal center. Therefore, in order for cysteine sulfinic acid products to form the sulfoxide has to rebind to the metal prior to the second oxygen atom transfer to give products, hence a much larger barrier than that obtained for the WT is found. Sulfoxide is released from the metal in $^5\mathbf{D}_A$ because the sulfoxide group experiences repulsion from the negatively charged axial acetate group. As a consequence, the rotation leads to a destabilized geometry in the H86D mutant and as a result the Fe−S bond breaks. Moreover, the electron transfer that takes place in the WT system from $^5\mathbf{C}_{WT}$ to $^5\mathbf{D}_{WT}$ is missing in the H86D mutant, hence the electronic descriptions of $^5\mathbf{C}_A$ and $^5\mathbf{D}_A$ are the same. Although mutation of one of the histidine side chains with aspartate influences barrier heights and consequently rate constants, the exothermicity of the overall reaction remains virtually the same and about 52 kcal mol^{-1} in energy is released in the process.

The potential energy profile of the H88D mutant shows that all barriers are increased in energy with respect to the WT system. The rate determining step shifts from dioxygen activation in WT to the second oxygen atom transfer reaction via $^5\mathbf{TS}_{DM}$. This barrier is almost equal in height to its precursor in the catalytic cycle, $^5\mathbf{TS}_{CM}$. These large barriers along the reaction mechanism may give all intermediates a relatively long lifetime and make the overall reaction slower. O−O bond breaking gives an iron−oxo species and cysteinyl oxide radical, but the latter is only bound to the metal with the amino group while the sulfoxide group is freely rotating. The oxo group is located trans to the carboxylic acid group and the sixth binding site is vacant. To proceed with the dioxygenation process the sulfoxide group of the cysteinyl oxide radical has to rebound to the iron and that will require the oxo group to rotate 90° and make space for the sulfoxide group. This structural rearrangement is energetically costly hence a barrier of 13.8 kcal mol^{-1} is encountered in this process. Thus, it may very well be that the sulfoxide intermediate is the end product of the H88D mutant reaction and that cysteine sulfoxide byproduct will be observed or alternatively lead to inactivation of the enzyme. The final oxygen atom transfer was found to be almost barrierless for WT but now encounters a significant barrier of 14.3 kcal mol^{-1}. Although, the sulfur group is accessible to the second oxygen atom, binding of the sulfinic acid group as a bidentate ligand is unfavorable due to the push effect of electrons of the carboxylic acid group trans to the sulfinic acid moiety. Therefore, the final oxygen atom transfer results in breaking of the Fe−OS bond and formation of a new Fe−O bond. In summary, the H88D mutant will be a much less efficient catalyst of dioxygenation reactions as it weakens thiolate binding to the iron center and triggers release of cysteine sulfoxide byproduct.

The axial ligand trans to the dioxygen group in **A** is replaced by a carboxylic acid group in the H86D mutant. In heme enzymes it has been shown that the axial ligand can either push or pull electrons from the iron center and influence catalytic properties.[39] In particular, peroxidases tend to have a histidine axial ligand while monoxygenase enzymes such as cytochrome P450 and nitric oxide synthase (NOS) have a cysteinate axial ligand.[1,40,41] A histidine ligand is proposed to entice a pull effect of electrons whereas an anionic ligand such as cysteinate gives a push effect on the iron−oxo group.[42] DFT studies that addressed the axial ligand effect on regioselective alkyl group hydroxylation versus C=C epoxidation showed that the rate constants of substrate monoxygenation are determined by the nature of the axial ligand.[43] The studies presented in this work focus on the ligand effects of nonheme systems.

The studies on H86D−CDO predict that the rate determining step in the catalytic cycle is the dioxygen bond breaking via barrier $^5\mathbf{TS}_{BA}$ of 14.2 kcal mol^{-1}. In WT $^5\mathbf{TS}_B$ both oxygen atoms have significant spin density but in opposite direction ($\rho_{O1} = 0.53$; $\rho_{O2} = -0.48$), which means the two electrons are in a singlet spin orientation and a homolytic bond breaking will lead to two radicals, one on each oxygen atom. By contrast, in the mutants bond breaking is heterolytic and for instance in $^5\mathbf{TS}_{BA}$ the spin densities on the two oxygen atoms are aligned and an electron transfer is required to break the bond to give a cysteinyl sulfoxide. Interestingly, the cysteinyl sulfoxide system is considerably stabilized with respect to the energy of WT. However, reorientation of the cysteinyl sulfoxide leads to breaking of the Fe−S bond but in contrast to WT the system fails to rebind the cysteinyl sulfoxide via the Fe−O bond. Therefore, a considerable barrier is required for the final oxygen atom transfer to form cysteine sulfinic acid products. In summary, since the dioxygenation reaction takes place in a plane perpendicular to the O−Fe−O axis in the H86D mutant, the initial steps in the reaction cycle resemble those for the WT system closely. However, the iron−oxo species ($^5\mathbf{C}_A$) is considerably stabilized with respect to WT due to the push effect of the axial ligand. Stabilization of the iron−oxo species does not lead to lower reaction barriers for the subsequent oxygen atom transfer step but raises barrier heights instead. This observation is in line with experimental studies of the axial ligand effect of nonheme iron−oxo complexes that showed that the least stable complexes give the highest reactivities.[18a]

Electronic Differences of Iron−Oxo Complexes in WT and Mutants. Group spin charges of the iron−oxo species ($^5\mathbf{D}$) of WT, H86D, and H88D are shown in Figure 10. Although the charge on the metal shows little effect of the ligands bound to it, there is a dramatic change in charge on the oxo group. Thus, in WT as well as H88D mutant the charge on the oxo group is −0.29 and −0.23, respectively, but using an anionic axial ligand as in H86D−CDO the charge on the oxo group is enhanced to −0.62. Therefore, the push effect of the axial ligand makes the oxo group more negative. An analogous effect is observed in the H88D mutant, where the group trans to the acetate group, i.e., the sulfoxide group, gains significant negative charge, in this case a change from $Q_{CysO} = -0.57$ in WT to $Q_{CysO} = -1.11$ in the mutant is observed. This enhanced negative charge of the sulfoxide group has dramatic effects on the second oxygen atom transfer reaction barrier ($^5\mathbf{TS}_{DM}$), which is considerably destabilized and now rate determining. Charges on all other groups show little influence as a result of site directed mutations, consequently we only find evidence of trans-effects of ligands bound to a metal center, whereas cis-effects of ligands perpendicular to each other on a metal center appear to be negligible.

Conclusion

Density functional calculations on an active site model of cysteine dioxygenase and two mutants with a 2His/1Asp bound motif have been studied. The results show that the 3His motif in CDO is essential for catalytic activity to form cysteine sulfinic acid products efficiently. The exothermicity of the reaction is not influenced by these mutations, but the reaction barriers for the individual steps in the reaction cycle are strongly influenced. In particular, a mutation trans to the dioxygen moiety, i.e., in the axial ligand position, results in increased O−O bond

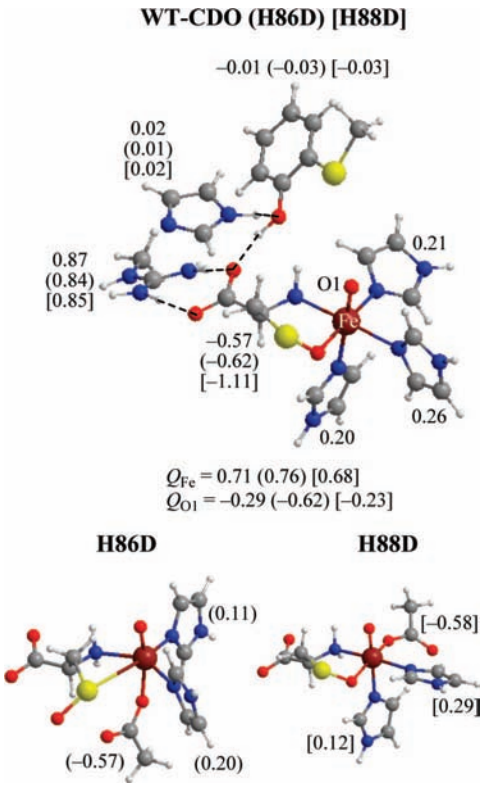

Figure 10. Group charges of iron−oxo complexes of WT CDO and two His/Asp mutants studied here.

breaking barriers. Although effects of substitution of ligands perpendicular to the Fe−O_2 bond are expected to be small, in CDO they are considerable due to a cysteinate sulfur atom trans to the group. The push effect of an acetate group trans to the cysteine group influences the Fe−S bond strength strongly and increases the barrier heights of reaction.

Acknowledgment. The National Service of Computational Chemistry Software (NSCCS) is acknowledged for providing generous CPU time.

Supporting Information Available: Six tables with group spin densities, charges and relative energies of all complexes described in this work, as well as eight figures with geometry scans, twelve figures with detailed optimized geometries of all critical points, and Cartesian coordinates of all structures described here. This material is available free of charge via the Internet at http://pubs.acs.org.

References and Notes

(1) (a) Sono, M.; Roach, M. P.; Coulter, E. D.; Dawson, J. H. *Chem. Rev.* **1996**, *96*, 2841–2888. (b) Kadish, K. M., Smith, K. M., Guilard, R., Eds. *The Porphyrin Handbook*; Academic Press: San Diego, CA, 2000. (c) Groves, J. T. *Proc. Natl. Acad. Sci. U.S.A.* **2003**, *100*, 3569–3574. (d) Guengerich, F. P. *Chem. Res. Toxicol.* **2001**, *14*, 611–650. (e) Ortiz de Montellano, P. R., Ed. *Cytochrome P450: Structure, Mechanism and Biochemistry*, 3rd ed.; Kluwer Academic/Plenum Publishers: New York, 2004. (f) Munro, A. W.; Girvan, H. M.; McLean, K. J. *Nat. Prod. Rep.* **2007**, *24*, 585–609.

(2) (a) Solomon, E. I.; Brunold, T. C.; Davis, M. I.; Kemsley, J. N.; Lee, S.-K.; Lehnert, N.; Neese, F.; Skulan, A. J.; Yang, Y.-S.; Zhou, J. *Chem. Rev.* **2000**, *100*, 235–349. (b) Bugg, T. D. H. *Tetrahedron* **2003**, *59*, 7075–7101. (c) Costas, M.; Mehn, M. P.; Jensen, M. P.; Que, L., Jr. *Chem. Rev.* **2004**, *104*, 939–986.

(3) (a) Stipanuk, M. H. *Annu. Rev. Nutr.* **2004**, *24*, 539–577. (b) Straganz, G. D.; Nidetzky, B. *ChemBioChem* **2006**, *7*, 1536–1548. (c) Joseph, C. A.; Maroney, M. J. *Chem. Commun.* **2007**, 3338–3349.

(4) Heafield, M. T.; Fearn, S.; Steventon, G. B.; Waring, R. H.; Williams, A. C.; Sturman, S. G. *Neurosci. Lett.* **1990**, *110*, 216–220.

(5) Perry, T. L.; Norman, M. G.; Yong, V. W.; Whiting, S.; Crichton, J. U.; Hansen, S.; Kish, S. *J. Ann. Neurol.* **1985**, *18*, 482–489.

(6) (a) McCoy, J. G.; Bailey, L. J.; Bitto, E.; Bingman, C. A.; Aceti, D. J.; Fox, B. G.; Phillips, G. N., Jr. *Proc. Natl. Acad. Sci. U.S.A.* **2006**, *103*, 3084–3089. (b) Simmons, C. R.; Liu, Q.; Huang, Q.; Hao, Q.; Begley, T. P.; Karplus, P. A.; Stipanuk, M. H. *J. Biol. Chem.* **2006**, *281*, 18723–18733. (c) Pierce, B. D.; Gardner, J. D.; Bailey, L. J.; Brunold, T. C.; Fox, B. G. *Biochemistry* **2007**, *46*, 8569–8578.

(7) Ye, S.; Wu, X.; Wei, L.; Tang, D.; Sun, P.; Bartlam, M.; Rao, Z. *J. Biol. Chem.* **2007**, *282*, 3391–3402.

(8) Aluri, S.; de Visser, S. P. *J. Am. Chem. Soc.* **2007**, *129*, 14846–14847.

(9) Lombardini, J. B.; Singer, T. P.; Boyer, P. D. *J. Biol. Chem.* **1969**, *244*, 1172–1175.

(10) Dominy, J. E., Jr.; Hwang, J.; Guo, S.; Hirschberger, L. L.; Zhang, S.; Stipanuk, M. H. *J. Biol. Chem.* **2008**, *283*, 12188–12201.

(11) (a) Ryle, M. J.; Hausinger, R. P. *Curr. Opin. Chem. Biol.* **2002**, *6*, 193–201. (b) Bollinger, J. M., Jr.; Price, J. C.; Hoffart, L. M.; Barr, E. W.; Krebs, C. *Eur. J. Inorg. Chem.* **2005**, 4245–4254. (c) Abu-Omar, M. M.; Loaiza, A.; Hontzeas, N. *Chem. Rev.* **2005**, *105*, 2227–2252.

(12) (a) Choroba, O. W.; Williams, D. H.; Spencer, J. B. *J. Am. Chem. Soc.* **2000**, *122*, 5389–5390. (b) Higgins, L. J.; Yan, F.; Liu, P.; Liu, H.-W.; Drennan, C. L. *Nature* **2005**, *437*, 838–844.

(13) (a) Trewick, S. C.; Henshaw, T. F.; Hausinger, R. P.; Lindahl, T.; Sedgwick, B. *Nature* **2002**, *419*, 174–178. (b) Falnes, P. Ø.; Johansen, R. F.; Seeberg, E. *Nature* **2002**, *419*, 178–182. (c) Duncan, T.; Trewick, S. C.; Koivisto, P.; Bates, P. A.; Lindahl, T.; Sedgwick, B. *Proc. Natl. Acad. Sci. U.S.A.* **2002**, *99*, 16660–16665. (d) Aas, P. A.; Otterlei, M.; Falnes, P. Ø; Vågbø, C. B.; Skorpen, F.; Akbari, M.; Sundheim, O.; Bjørås, M.; Slupphaug, G.; Seeberg, E.; Krokan, H. E. *Nature* **2003**, *421*, 859–863. (e) Mishina, Y.; Duguid, E. M.; He, C. *Chem. Rev.* **2006**, *106*, 215–232.

(14) O'Brien, J. R.; Schuller, D. J.; Yang, V. S.; Dillard, B. D.; Lanzilotta, W. N. *Biochemistry* **2003**, *42*, 5547–5554.

(15) Que, L., Jr *Nat. Struct. Biol.* **2000**, *7*, 182–184.

(16) See for example: (a) Hegg, E. L.; Que, L., Jr *Eur. J. Biochem.* **1997**, *250*, 625–629. (b) Beck, A.; Barth, A.; Hübner, E.; Burzlaff, N. *Inorg. Chem.* **2003**, *42*, 7182–7188. (c) Oldenburg, P. D.; Shteinman, A. A.; Que, L., Jr. *J. Am. Chem. Soc.* **2005**, *127*, 15672–15673. (d) Oldenburg, P. D.; Ke, C.-Y.; Tipton, A.; Shteinman, A. A.; Que, L., Jr. *Angew. Chem., Int. Ed.* **2006**, *45*, 7975–7978. (e) Bruijnincx, P. C. A.; Lutz, M.; Spek, A. L.; Hagen, W. R.; Weckhuysen, B. M.; van Koten, G.; Klein Gebbink, R. J. M. *J. Am. Chem. Soc.* **2007**, *129*, 2275–2286. (f) Bruijnincx, P. C. A.; Buurmans, I. L. C.; Gosiewska, S.; Moelands, M. A. H.; Lutz, M.; Spek, A. L.; van Koten, G.; Klein Gebbink, R. J. M. *Chem. Eur. J.* **2008**, *14*, 1228–1237.

(17) (a) Kaizer, J.; Klinker, E. J.; Oh, N. Y.; Rohde, J.-U.; Song, W. J.; Stubna, A.; Kim, J.; Münck, E.; Nam, W.; Que, L., Jr. *Am. Chem. Soc.* **2004**, *126*, 472–473. (b) Oh, N. Y.; Suh, Y.; Park, M. J.; Seo, M. S.; Kim, J.; Nam, W. *Angew. Chem., Int. Ed.* **2005**, *44*, 4235–4239.

(18) (a) Sastri, C. V.; Park, M. J.; Ohta, T.; Jackson, T. A.; Stubna, A.; Seo, M. S.; Lee, J.; Kim, J.; Kitagawa, T.; Münck, E.; Que, L., Jr.; Nam, W. *J. Am. Chem. Soc.* **2005**, *127*, 12494–12495. (b) Nam, W. *Acc. Chem. Res.* **2007**, *40*, 522–531. (c) Hirao, H.; Que, L., Jr.; Nam, W.; Shaik, S. *Chem. Eur. J.* **2008**, *14*, 1740–1756.

(19) (a) Lim, M. H.; Rohde, J.-U.; Stubna, A.; Bukowski, M. R.; Costas, M.; Ho, R. Y. N.; Münck, E.; Nam, W.; Que, L., Jr. *Proc. Natl. Acad. Sci. U.S.A.* **2003**, *100*, 3665–3670. (b) Rohde, J.-U.; Stubna, A.; Bominaar, E.; Münck, E.; Nam, W.; Que, L., Jr *Inorg. Chem.* **2006**, *45*, 6435–6445.

(20) (a) Gross, Z.; Nimri, S. *Inorg. Chem.* **1994**, *33*, 1731–1732. (b) Czarnecki, K.; Nimri, S.; Gross, Z.; Proniewicz, L. M.; Kincaid, J. R. *J. Am. Chem. Soc.* **1996**, *118*, 2929–2935. (c) Nam, W.; Lim, M. H.; Oh, S.-Y.; Lee, J. H.; Lee, H. J.; Woo, S. K.; Kim, C.; Shin, W. *Angew. Chem., Int. Ed.* **2000**, *39*, 3646–3649. (d) Rohde, J.-U.; Que, L., Jr. *Angew. Chem., Int. Ed.* **2005**, *44*, 2255–2258.

(21) Grzyska, P. K.; Müller, T. A.; Campbell, M. G.; Hausinger, R. P. *J. Inorg. Biochem.* **2007**, *101*, 797–808.

(22) (a) Kreisberg-Zakarin, R.; Borovok, I.; Yanko, M.; Frolow, F.; Aharonowitz, Y.; Cohen, G. *Biophys. Chem.* **2000**, *86*, 109–118. (b) Fitzpatrick, P. F.; Ralph, E. C.; Ellis, H. R.; Wilmon, O. J.; Daubner, S. C. *Biochemistry* **2003**, *42*, 2081–2088.

(23) (a) de Visser, S. P. *Angew. Chem., Int. Ed.* **2006**, *45*, 1790–1793. (b) de Visser, S. P. *J. Am. Chem. Soc.* **2006**, *128*, 9813–9824. (c) de Visser, S. P. *Chem. Commun.* **2007**, 171–173. (d) de Visser, S. P.; Latifi, R. *J. Phys. Chem. B* **2009**, *113*, 12–14. (e) de Visser, S. P. *Coord. Chem. Rev.* **2009**. In press.

(24) (a) Becke, A. D. *J. Chem. Phys.* **1993**, *98*, 5648–5652. (b) Lee, C.; Yang, W.; Parr, R. G. *Phys. Rev. B* **1988**, *37*, 785–789.

(25) (a) de Visser, S. P.; Oh, K.; Han, A.-R.; Nam, W. *Inorg. Chem.* **2007**, *46*, 4632–4641. (b) Kumar, D.; de Visser, S. P.; Sharma, P. K.; Cohen, S.; Shaik, S. *J. Am. Chem. Soc.* **2004**, *126*, 1907–1920. (c) de Visser, S. P.;

Kumar, D.; Cohen, S.; Shacham, R.; Shaik, S. *J. Am. Chem. Soc.* **2004**, *126*, 8362–8363. (d) de Visser, S. P. *Chem. Eur. J.* **2006**, *12*, 8168–8177. (e) Shaik, S.; Kumar, D.; de Visser, S. P. *J. Am. Chem. Soc.* **2008**, *130*, 10128–10140.

(26) (a) Hay, P. J.; Wadt, W. R. *J. Chem. Phys.* **1985**, *82*, 270–283. (b) Hehre, W. J.; Ditchfield, R.; Pople, J. A. *J. Chem. Phys.* **1972**, *56*, 2257–2261.

(27) *Jaguar 7.0*; Schrödinger, LLC., New York, 2007.

(28) Frisch, M. J.; Trucks, G. W.; Schlegel, H. B.; Scuseria, G. E.; Robb, M. A.; Cheeseman, J. R.; Montgomery, J. A., Jr.; Vreven, T.; Kudin, K. N.; Burant, J. C.; Millam, J. M.; Iyengar, S. S.; Tomasi, J.; Barone, V.; Mennucci, B.; Cossi, M.; Scalmani, G.; Rega N.; Petersson, G. A.; Nakatsuji, H.; Hada, M.; Ehara, M.; Toyota, K.; Fukuda, R.; Hasegawa, J.; Ishida, M.; Nakajima, T.; Honda, Y.; Kitao, O.; Nakai, N.; Klene, M.; Li, X.; Knox, J. E.; Hratchian, H. P.; Cross, J. B.; Adamo, C.; Jaramillo, J.; Gomperts, R.; Stratmann, R. E.; Yazyev, O.; Austin, A. J.; Cammi, R.; Pomelli, C.; Ochterski, J. W.; Ayala, P. Y.; Morokuma, K.; Voth, G. A.; Salvador, P.; Dannenberg, J. J. ; Zakrzewski, V. G.; Dapprich, S.; Daniels, A. D.; Strain, M. C.; Farkas, O.; Malick, D. K.; Rabuck, A. D.; Raghavachari, K.; Foresman, J. B.; Ortiz, J. V.; Cui, Q.; Baboul, A. G.; Clifford, S; Cioslowski, J.; Stefanov, B. B.; Liu, G.; Liashenko, A.; Piskorz, P.; Komaromi, I.; Martin, R. L.; Fox, D. J.; Keith, T.; Al-Laham, M. A.; Peng, C. Y.; Nanayakkara, A.; Challacombe, M.; Gill, P. M. W.; Johnson, B.; Chen, W.; Wong, M. W.; Gonzalez, C.; Pople, J. A. *Gaussian03*, Revision C.01; Gaussian, Inc., Wallingford CT, 2004.

(29) (a) Siegbahn, P. E. M. *Q. Rev. Biophys.* **2003**, *36*, 91–145. (b) Godfrey, E.; Porro, C. S.; de Visser, S. P. *J. Phys. Chem. A* **2008**, *112*, 2464–2468.

(30) (a) Shaik, S.; de Visser, S. P.; Ogliaro, F.; Schwarz, H.; Schröder, D. *Curr. Opin. Chem. Biol.* **2002**, *6*, 556–567. (b) Shaik, S.; Kumar, D.; de Visser, S. P.; Altun, A.; Thiel, W. *Chem. Rev.* **2005**, *105*, 2279–2328.

(31) Straganz, G. D.; Nidetzky, B. *J. Am. Chem. Soc.* **2005**, *127*, 12306–12314.

(32) Sinnecker, S.; Svensen, N.; Barr, E. W.; Ye, S.; Bollinger, J. M., Jr.; Neese, F.; Krebs, C. *J. Am. Chem. Soc.* **2007**, *129*, 6168–6179.

(33) Choudhury, K.; Sundaramoorthy, M.; Hickman, A.; Yonetani, T.; Woehl, E.; Dunn, M. F.; Poulos, T. L. *J. Biol. Chem.* **1994**, *269*, 20239–20249.

(34) Costas, M.; Que, L., Jr *Angew. Chem., Int. Ed* **2001**, *41*, 2179–2181.

(35) (a) Lundberg, M.; Morokuma, K. *J. Phys. Chem. B* **2007**, *111*, 9380–9389. (b) Lundberg, M.; Siegbahn, P. E. M.; Morokuma, K. *Biochemistry* **2008**, *47*, 1031–1042.

(36) (a) Zhou, Y.; Shan, X.; Mas-Ballesté, R.; Bukowski, M. R.; Stubna, A.; Chakrabarti, M.; Slominski, L.; Halfen, J. A.; Münck, E.; Que, L., Jr. *Angew. Chem., Int. Ed.* **2008**, *47*, 1896–1899. (b) de Visser, S. P.; Nam, W. *J. Phys. Chem. A* **2008**, *112*, 12887–12895.

(37) Sastri, C. V.; Lee, J.; Oh, K.; Lee, Y. J.; Lee, J.; Jackson, T. A.; Ray, K.; Hirao, H.; Shin, W.; Halfen, J. A.; Kim, J.; Que, L., Jr.; Shaik, S.; Nam, W. *Proc. Natl. Acad. Sci. U.S.A.* **2007**, *104*, 19181–19186.

(38) Borowski, T.; Bassan, A.; Siegbahn, P. E. M. *Chem. Eur. J.* **2004**, *10*, 1031–1041.

(39) (a) Dawson, J. H.; Holm, R. H.; Trudell, J. R.; Barth, G.; Linder, R. E.; Bunnenberg, E.; Djerassi, C.; Tang, S. C. *J. Am. Chem. Soc.* **1976**, *98*, 3707–3709. (b) Poulos, T. L. *J. Biol. Inorg. Chem.* **1996**, *1*, 356–359. (c) Ogliaro, F.; de Visser, S. P.; Shaik, S. *J. Inorg. Biochem.* **2002**, *91*, 554–567.

(40) (a) Veitch, N. C.; Smith, A. T. *Adv. Inorg. Chem.* **2000**, *51*, 107–162. (b) Berglund, G. I.; Carlsson, G. H.; Smith, A. T.; Szöke, H.; Henriksen, A.; Hajdu, J. *Nature* **2002**, *417*, 463–468. (c) Nicholls, P.; Fita, I.; Loewen, P. C. *Adv. Inorg. Chem.* **2000**, *51*, 51–106.

(41) (a) Groves, J. T.; Wang, C. C.-Y. *Curr. Opin. Chem. Biol.* **2000**, *4*, 687–695. (b) Poulos, T. L.; Li, H.; Raman, C. S.; Schuller, D. J. *Adv. Inorg. Chem.* **2000**, *51*, 243–294. (c) Stuehr, D. J.; Wei, C.-C.; Wang, Z.; Hille, R. *Dalton Trans.* **2005**, 3427–3435. (d) de Visser, S. P.; Tan, L. S. *J. Am. Chem. Soc.* **2008**, *130*, 12961–12974.

(42) (a) de Visser, S. P.; Shaik, S.; Sharma, P. K.; Kumar, D.; Thiel, W. *J. Am. Chem. Soc.* **2003**, *125*, 15779–15788. (b) Kumar, D.; de Visser, S. P.; Sharma, P. K.; Hirao, H.; Shaik, S. *Biochemistry* **2005**, *44*, 8148–8158. (c) Wang, R.; de Visser, S. P. *J. Inorg. Biochem.* **2007**, *101*, 1464–1472.

(43) (a) de Visser, S. P.; Ogliaro, F.; Sharma, P. K.; Shaik, S. *Angew. Chem. Int. Ed* **2002**, *41*, 1947–1951; *Angew. Chem.* **2002**, *114*, 2027−2031. (b) de Visser, S. P.; Ogliaro, F.; Sharma, P. K.; Shaik, S. *J. Am. Chem. Soc.* **2002**, *124*, 11809–11826. (c) Kumar, D.; de Visser, S. P.; Sharma, P. K.; Derat, E.; Shaik, S. *J. Biol. Inorg. Chem.* **2005**, *10*, 181–189.

JP809700F